Sixth International Symposium on Marine Propulsors
smp'19, Rome, Italy, May 2019

Pre-Swirl Fins Adapted to Different Operation Conditions

Jens Ring Nielsen[1], Wei Jin[1]

[1]MAN Energy Solutions, Frederikshavn, Denmark

ABSTRACT

This paper deals with the invention of Controllable Pre-Swirl Fins (CPSF) placed in front of the propeller and arranged in such a way that they can be adapted to different operating conditions by optimizing their pitch and flap settings. The CFD software STAR CCM+ has been used to derive the hydrodynamic performance of a matrix of different number of fin configurations in full scale both at design and ballast drafts. Subsequently, the model scale optimizations were carried out based on the full scale optimum. The CFD model scale optimization results were then validated against an extensive and dedicated series of model tests in a towing tank. The obtained optimal pitch angles at the two conditions were then averaged and kept fixed for the remaining part of the tests. The subsequent tests were used to determine the optimum flap angles, again for each of the two conditions. Generally, the CFD determined optimal fin pitch angles were well validated by the tank tests, while the optimum flap angles were in less agreement. It proved that the CPSF could lead to savings of the delivered shaft power by about 3-4% in case of the selected bulk carrier at both conditions.

Keywords

Controllable Pre-Swirl Fins (CPSF), Energy Saving Device (ESD), CFD Optimization, Full and Model Scale.

1 INTRODUCTION

It is always a key focus point in the shipping industry to save on fuel consumption and reduce emissions. Furthermore, strict regulations as to the emission from ships and the implementation of Energy Efficiency Design Index (EEDI) are the main drivers for researches, ship designers and propulsion system suppliers for developing hydrodynamic Energy Saving Devices (ESD) for ships. Hydrodynamic ESD has been widely accepted as an important way to lower the fuel consumptions and the pollutant emission, both for new buildings and retrofits. For its simplicity in design and effectiveness in operation, Pre-Swirl Stators (PSS) has drawn great attentions from ship research agencies and industries, as published by Kim et al (2004) and Nielsen et al (2013).

However, just as hinted in its name, PSS is a set of fixed fins in front of the propeller. This determines that PSS could only be optimized at a specific load condition. Thus, a set of fins located upstream of the propeller, which has the same effect as PSS and can also be adapted to different operation conditions (draft, speed, fouling, sea and weather) means better performance at different states. This became the initiative of the Blue INNOship Controllable Pre-Swirl Fins (CPSF) Project. The aim of CPSF Project is to develop a set of controllable swirl fins upstream of the propeller by improving the working environment of the propeller at different operation conditions. The benefits from this will be fuel oil savings and consequently lower emissions, possibly lower noise and cavitation level.

2 GEOMETRIES DESCRIPTION

According to the project plan, a 32 500 DWT bulk carrier was selected as the objective for the CPSF optimization. A single 4-blade right-handed fixed pitch propeller propels the vessel. The dimensions and particulars are listed in Table 1. Figure 1 shows the ship and propeller models manufactured by FORCE Technology.

			Ship	Model
Length	L_{pp}	m	171.506	7.685
Breadth	B	m	28.4	1.273
Design Draft	T	m	10	0.448
Volume at Design	V	m^3	39960.85	3.595
Wetted Surface at Design	S	m^2	7234.18	14.524
Blade Diameter	D	m	5.2	0.233
Area Ratio	A_e/A_0		0.502	
Blade Number			4	

Table 1 Particulars of Hull and Propeller

Figure 1 Hull and Propeller Models of the Bulk Carrier

3 CFD TOOL DESCRIPTION

During the validation and optimization stages, the commercial CFD software STAR CCM+ was used to calculate the hull and fins resistance, propeller thrust and torque. In order to achieve quick and stable results, the wave making resistance was calculated using VOF method, only in the bare hull situation. Then a second bare hull resistance was calculated using a dummy model, i.e., the free surface was not included. The difference of these two resistance calculations was considered as the wave making resistance at each condition. In the following optimization stages at this condition, all self-propulsions were calculated with dummy model. The previously obtained wave making resistance was then added to the resistance without free surface to obtain the total resistance. The influence of the CPSF on the free surface was considered ignorable. For the reason that the sinkage and trim data were not initially available, they are not considered during the validation and all the optimization stages. The relatively simpler but robust two-equation SST k-w turbulence model was adopted to capture the turbulent flow, with wall function to bridge the near wall laminar sub-layer to the completely turbulent area. The rotation of the propeller was firstly simulated using the quick but not very accurate method, Moving Reference Frame (MRF) model to get the initial data. Then the Rigid Body Motion (RBM) model was activated from the converged initial MRF result. The RBM model is more time consuming but the most precise way to capture the interaction of the hull, fins and propeller. By doing so, good accuracy can be obtained in a relatively quick way. To make the large amount of optimization calculations feasible, we used a modest mesh with about 3.2 million cells, among which 1.6 million were applied at the MRF or RBM region around this 4-blade propeller. What's more, the time step size was fixed at 6 degrees blade rotation angle to accelerate the converge process. According to the authors' experience, if the mesh size and time step, including the adopted turbulence model, are finer, then the accuracy will be better. The mesh and solver configurations mentioned above were adopted both in model and in full scale as a trade-off between computational accuracy and speed.

4 PROCEDURES OF THE OPTIMIZATIONS

According to the project's plan, the general work packages comprising concept study and development and testing were distributed among the four partners in close cooperation. Apart from the CFD optimization and development of the fins described in this paper, a mechanical design including fin actuation forms a part of the project as well.

In order to make the CPSF work most optimally at both design and ballast conditions, a flap version of CPSF was finally selected due to its simplicity in mechanical design and actuation. Each fin includes two parts: a fixed part and a flapped part. Thus, the CFD optimization will be done according to the following procedures:

1) Find design condition's optimal pitches for each fin.

2) Independence tests of fins at design condition.

3) Find ballast condition's optimal pitches for each fin.

4) Independence tests of fins at ballast condition.

5) Average the optimal pitch for the two conditions and apply it to the fix part of these two conditions.

6) Optimize the flap angles at these two conditions.

The optimization started from full scale, which was followed by a series of model scale optimization. The latter was used as an initial setting of the individual fin's pitch and flap during the subsequent model testing. A set of fins covering the range for different flap deflections were milled and used for verification of the CFD analysis and tested at the towing tank.

5 CPSF GEOMETRY

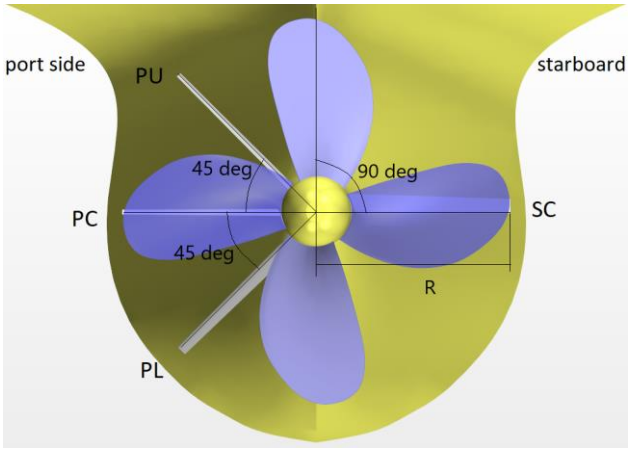

Figure 2 Fins distribution for the right handed propeller

The fins' angular distribution follows a similar setting as used by Kim et al (2013), thus three fins at the portside and one fin at starboard side, for the right-handed rotation propeller, as shown in Figure 2. PU, PC and PL are the portside upper, center and lower fin respectively and SC is the starboard side center fin. Assuming that 12 O'clock is 0 degree and clockwise is positive angle direction, then

SC=90° PL=225° PC=270° PU=315°

The length of the fins is kept the same as the propeller radius R. Fin profile selected is of the NACA66-x10 series. The camber height (x) will be added to the symmetrical profile to get the cambered fins. Figure 3 shows the definitions of camber application. Furthermore, the fins are tapered with a chord length of 0.3R at the base and 0.2R at the tip. Where the fins intersects the hull, they are faired to follow the hull curvature. The fin includes a fix part (60% of the chord) and a flap part (40% of the chord). The flap part is designed to be rotatable to adapt to different ship operation conditions.

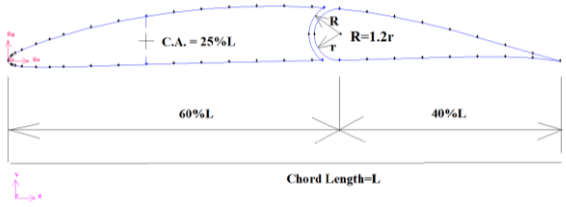

Figure 3 Fin with Positive camber of 5% Chord Length

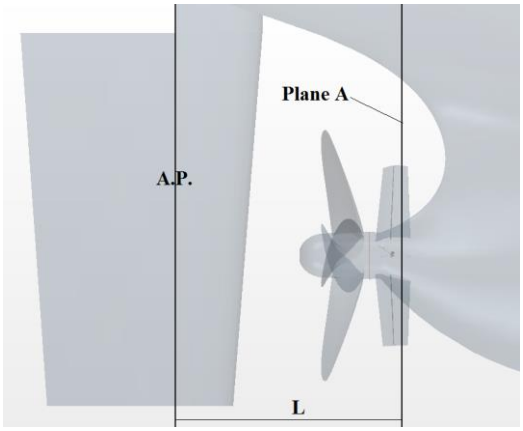

Figure 4 Location of the Fins

Figure 4 presents the relative longitudinal position of the fins with the propeller plane. Plane A is the plane going through aerodynamic center of all fin profiles. Plane A is located upstream of the propeller plane with a distance of 0.425R. Thus L = propeller position from A.P. + 0.425R.

6 RESULTS OF CFD ANALYSIS

6.1 Full scale validation

For the reason that the reference data obtained at the start of the project were given only in full scale, the validation could thus only be carried out accordingly. This includes the bare hull resistance, open water curve of the propeller, and the self-propulsion's extrapolated full scale results from model tests.

As is known in RANS simulation, Y+ value, which is related to the mesh height closest to the wall, together with the wall treatment, determines how the transition is from the near wall flow to the fully turbulent flow. Thus, a series of Y+ values were tested by tuning the prism layer number and stretching ratio at the design bare hull condition. Generally, all the tested mean Y+ values from 750 to 3000 could guarantee the deviations to be within 2%. Even though the first layer mesh is located out of the log-law layer, the full scale bare hull resistance can be well predicted using the adopted mesh configuration. As to the propeller, the open water data was calculated using the turbulence model without transition. Only one blade passage computational domain was built. After several rounds of test, a 2.2 million mesh setup with a mean Y+ around 93 was adopted to secure sufficient accuracy without introducing a too high computation cost in full scale. The ship and propeller were then assembled to make the self-propulsion validation. During this process, RPS was tuned to get the equilibrium, namely, the hull resistance with propeller is very close to the propeller thrust. We set the relative deviation limit to be 0.01%.

Self-Propulsion	η_O	η_R	η_H	η_D	P_{DB} (W)
CFD	0.5469	1.0309	1.1518	0.6494	4779461
FORCE	0.5370	1.0200	1.2190	0.6680	4791622
Dev (%)	1.85	1.07	-5.52	-2.78	-0.25

Table 2 Validation of the Propulsion Factors

Table 2 is the validation of the propulsion factors. Generally, the accuracy is very good. We applied this standard solver configuration for the following CPSF optimizations.

6.2 Full scale optimization

According to the selected bulk carrier's log data between 2015 and 2016, two operation conditions appeared typically in Table 3. All the following optimizations both in full and model scale were based on these two distinctive conditions - design and ballast.

Condition		Design	Ballast
Fore Draft	m	10.0	5.0
Aft Draft	m	10.0	7.0
Mean Draft	m	10.0	6.0
Trim	m	0.0	2.0
Ship Speed	kn	11.5	12.0

Table 3 Optimization Conditions

For the full scale optimizations, we firstly selected the symmetrical (no camber) fin to optimize the pitch angles. Only one fin was optimized each time, with the other three fins at 0 degree pitch angle. The angle interval is set to be 2 degrees. It can be expected that if these optimized best angles combined together, too much pre-swirl will be generated. Thus, an independence test was followed. This is realized by means of tuning each fin a range of pitch angles, based on the best combination of each fin. After one fin reaching the minimum required shaft power, then keep the best pitch angle and continue to the next fin. Finally, the optimal set of pre-swirl fins are obtained. The same procedures were applied to the positive camber (Figure 3) fin and negative camber fin, both in design and ballast conditions. To make the difference with the symmetrical fins, the cambered fins were named as CPC, CPL, CPU and CSC.

	Design Condition	Saving (%)	Ballast Condition	Saving (%)
	SP (No Fins)	-	SP (No Fins)	-
	Best Pitch Angle	Saving (%)	Best Pitch Angle	Saving (%)
	+8PC	-0.09	+6PC	-0.32
	-2PL	0.11	-8PL	-0.59
No Camber	+2PU	0.16	+4PU	-0.46
	-18SC	-1.34	-18SC	-1.04
	SUM	-1.16	SUM	-2.41
Combination	+8PC-2PL+2PU-18SC	-1.15	+6PC-8PL+4PU-18SC	-1.24
Independent	0PC-2PL-2PU-18SC	-1.39	-2PC-20PL-2PU-20SC	-1.64
	Best Pitch Angle	Saving (%)	Best Pitch Angle	Saving (%)
	+4CPC	-0.09	-4CPC	-0.40
	-6CPL	-0.16	-8CPL	-0.97
5% Camber	+6CPU	-0.20	+2CPU	-0.30
	-22CSC	-1.37	-16CSC	-1.24
	SUM	-1.83	SUM	-2.91
Combination	+4CPC-6CPL+6CPU-22CSC	-1.55	-4CPC-8CPL+2CPU-16CSC	-2.33
Independent	0CPC-2CPL-4CPU-20CSC	-2.06	-4CPC-10CPL+2CPU-16CSC	-2.44

Table 4 Full Scale's Optimization Results without Flap

From Table 4, the following conclusions can be drawn:

1) Fins interact with each other, especially these three fins at portside.

2) Positive camber is better than negative camber during the optimization process. Thus, only positive camber's results were listed. The 5% camber is better than the symmetry fins by saving the shaft power about 0.8%.

3) The final independent fin configuration at design condition is even better than the sum of each fin's energy saving. On the contrary, at ballast condition, the final independent fin configuration has lower energy saving than the sum of each fin's energy saving.

4) At all situations, the starboard central fin obviously contributes most to the energy saving.

Then the averaged pitch angle of each fin at these two conditions was determined. Based on the averaged pitch angle fins, the optimal flap angles for each fin were obtained. Because of the mechanical limitations, the flap angle was fixed between ± (8 to10) degrees. To distinguish the difference between fixed fins and flapped ones the latter were named as FPC, FPL, FPU and FSC.

	Design Condition					Ballast Condition				
Full Scale	CPC	CPL	CPU	CSC	Saving (%)	CPC	CPL	CPU	CSC	Saving (%)
SP	No Fins				-	No Fins				-
No Camber	0	0	0	0	0.21	0	0	0	0	-0.31
5% Camber	0	0	0	0	-0.56	0	0	0	0	-1.03
Optimal Pitch Angle	0	-2	-4	-20	-2.06	-4	-10	2	-16	-2.44
At Different Condition	-4	-10	2	-16	-1.26	0	-2	-4	-20	-1.79
Averaged Pitch Angle	-2	-6	-2	-18	-1.76	-2	-6	-2	-18	-2.20
With Flap Angle	FPC	FPL	FPU	FSC		FPC	FPL	FPU	FSC	
Best Flap Angle	2	2	-6	-4	-2.13	-8	-10	2	-8	-2.70

Table 5 Full Scale Optimization and Comparison of CPSF

Table 5 summarizes the optimization and comparison results of fins with flap angles, both at design and ballast conditions in full scale. From Table 5, the following conclusions can be drawn:

1) Symmetrical fin with 0 pitch angle does not always result in energy savings. Similar with the previously obtained conclusion, 5% camber is better than the symmetry fins by an additional saving of about approx. 0.8%, compared with that at 0 pitch angle situation.

2) Averaged pitch angle with 0 flap angle gives about 0.2% to 0.3% lower energy saving compared to the optimal pitch angle with 0 flap angle cases.

3) Cross comparison shows if the optimal fins at one condition applied to the other, the energy saving is lower than the averaged pitch angle.

4) Averaged pitch angle for the fix part combining with the best flap angle gives the highest energy saving. This means that the flap scheme works better than the optimal configuration at each condition.

5) The deviations of the flap angles at the two conditions - design and ballast - are 10/12/8/4 degrees. Flap can help to improve about 0.5% energy saving compared with the averaged fixed fins.

6) For most of the cases, the flap part has obviously trend to rectify the whole fin to the optimal pitch angle without flap in the corresponding conditions. This means that the developed CPSF has obvious superiority over the PSS in hydrodynamics regard.

Full Scale									
Design Condition	Resistance (N)	RPS	1-t	1-w	η_O	η_R	η_H	η_D	P_{DB} (W)
SP	310459	1.8660	0.8111	0.7030	0.5470	1.0303	1.1537	0.6502	2827613
SP-CPSF	314102	1.8080	0.7923	0.6212	0.5160	1.0194	1.2756	0.6710	2767358
Dev (%)	1.17	-3.11	-2.31	-11.65	-5.66	-1.06	10.56	3.20	-2.13
Ballast Condition	Resistance (N)	RPS	1-t	1-w	η_O	η_R	η_H	η_D	P_{DB} (W)
SP	287854	1.8112	0.8185	0.6678	0.5536	1.0279	1.2258	0.6975	2550176
SP-CPSF	288416	1.7529	0.7913	0.5900	0.5237	1.0219	1.3411	0.7177	2481436
Dev (%)	0.20	-3.22	-3.33	-11.64	-5.41	-0.59	9.41	2.88	-2.70

Model Scale									
Design Condition	Resistance (N)	RPS	1-t	1-w	η_O	η_R	η_H	η_D	P_{DB} (W)
SP	44.7574	7.9482	0.7960	0.5960	0.5266	0.9571	1.3356	0.6731	43.2272
SP-CPSF	44.8562	7.7732	0.7813	0.5436	0.5023	0.9557	1.4374	0.6899	42.2382
Dev (%)	0.22	-2.20	-1.84	-8.79	-4.61	-0.15	7.62	2.51	-2.29
Ballast Condition	Resistance (N)	RPS	1-t	1-w	η_O	η_R	η_H	η_D	P_{DB} (W)
SP	39.648	7.5976	0.7946	0.5300	0.5164	0.9523	1.4992	0.7372	38.6585
SP-CPSF	39.6131	7.4078	0.7691	0.4714	0.4839	0.9506	1.6313	0.7505	37.7926
Dev (%)	-0.09	-2.50	-3.21	-11.05	-6.28	-0.18	8.82	1.80	-2.24

Table 6 Propulsion Factors Comparison

Table 6 lists the comparison of the propulsion factors both in full and model scales at design and ballast conditions. The following conclusions can be drawn:

1) At the bare hull condition, without propeller running, CPSF will generally increase the resistance. However, bare hull resistance with CPSF at ballast condition in model scale is a little lower than that without CPSF.

2) At all conditions, RPS is reduced with CPSF by 2.5% to 3% (full scale: about 3%, model scale: about 2.5%). The thrust of the propeller under the new equilibrium point with CPSF increases about 3% for all cases. However, the torque of the propeller for all cases does not change a lot. This makes the required shaft power a little lower. The energy saving for all cases is around 2% to 3%.

3) For all cases, the propeller efficiency behind the hull, η_B, reduces (5% to 6.5%) but hull efficiency increases more (8% to 10%). The relative rotation efficiency η_R does not reduce a lot, around 1% at full scale. Thus, the total propulsion efficiency η_D increases about 2% to 3%.

6.3 Model scale optimization

According to the conclusions obtained in full scale, the fins optimizations were carried out in model scale to obtain the best pitch setting of the fins and range of flap settings for the subsequent tank tests. The 5% positive camber was applied, as the best energy saving at full scale. Model scale's solver configurations were just scaled down from the full scale. The Y+ value of the hull was limited to 100. There were no model test data available for validation before the tank tests. Thus, the absolute deviation is not checked. However, it can be found that the relative difference between self-propulsion without and with CPSF is already shown in Table 6. This means that the results calculated using this solver configuration could be comparable for the following model scale optimization.

	Design Condition					Ballast Condition				
Model Scale	CPC	CPL	CPU	CSC	Saving (%)	CPC	CPL	CPU	CSC	Saving (%)
SP	No Fins				-	No Fins				-
Optimal Pitch Angle	4	-6	-10	-30	-2.60	-14	-20	-14	-18	-2.84
At Different Condition	-14	-20	-14	-18	-1.30	4	-6	-10	-30	-1.25
Averaged Pitch Angle	-5	-11	-12	-24	-1.87	-5	-11	-12	-24	-2.19
With Flap Angle	FPC	FPL	FPU	FSC		FPC	FPL	FPU	FSC	
Best Flap Angle	2	-8	0	0	-2.24	-8	-10	-8	0	-2.54

Table 7 Model Scale Optimization and Comparison

Table 7 summarizes the optimization and comparison results of fins with flap angle, both at design and ballast conditions in model scale. From Table 7, the following conclusions can be drawn:

1) Averaged pitch angle with 0 flap angle gives about 0.7% lower energy saving compared with the optimal pitch angle with 0 flap angle cases.

2) Cross comparison shows if the optimal fins at one condition applied to the other, the energy saving is lower than the averaged pitch angle.

3) Averaged pitch angle for the fix part combining with the best flap angle cannot save as much as the respective optimal pitch angle conditions.

4) The deviations of the flap angles at the two conditions - design and ballast - are 10/2/8/0 degrees. Flap can help to improve the energy saving about 0.5% compared with the averaged fixed fins.

5) Even though not so obvious, the flap part still presents some tendency to rectify the whole fin to the optimal pitch angle without flap in the corresponding conditions.

By comparing the optimization results and conclusions of full scale and model scale, the following main difference can be found:

1) At full scale, averaged pitch angle for the fix part combining with the best flap angle gives the highest energy saving, which is even higher than the optimal pitch angle without flap angle at the corresponding condition. However, at model scale, averaged pitch angle for the fix part combining with the best flap angle cannot save as high as the respective optimal pitch angle conditions.

2) If looking at the optimal pitch angle with 0 degree flap angle, we can find that every pitch angle at full scale is less than found at model scale. This should relate mainly to the scale effect of the boundary layer and the induced wake field.

From the differences between model and full scale, a clear scale effect can be noted. Thus, full scale is recommended for the CFD optimization of ESD like CPSF.

7 MODEL TEST VERIFICATION

The scope of the tank test at FORCE Technology included resistance, self-propulsion, wake measurement and CPSF optimization. The purpose of the CPSF optimization program is to determine the optimum fins and flaps angles of the device for a given speed and condition, and to compare the results of the final configuration to "the base case" model without CPSF, for a given range of speeds and the two drafts – design and ballast. For optimization tests, optimum configuration is defined as the configuration where required propeller power is at minimum relative to the reference case. The tests were carried out between 9 July and 20 July 2018 in the towing tank at FORCE Technology.

7.1 Description of test procedure

The optimal pitch angles were first obtained at design and ballast conditions. Then the average values of them were used as fixed pitch angles during the remaining tests. The flap angles at design and ballast condition were then optimized after its pitch angles optimization. Finally the CPC, CPL, CPU and CSC fin was removed one by one to test the different contribution to the total energy saving at ballast and design conditions.

7.2 Results and comparisons with CFD

The previously obtained pitch angles by CFD were regarded as the base for the tank tests angle setting to determine the optimal target pitch angles in an efficient way. Please note that during model tests a 5 degrees interval was adopted, instead of the 2 degrees during the CFD optimization stage. This consideration was made to cover a larger range of pitch and flap settings as experienced during the CFD optimization in model scale.

Model Scale-FORCE					Model Scale-CFD				
Optimal Pitch Angle (deg)					Optimal Pitch Angle (deg)				
Condition	CPC	CPL	CPU	CSC	Condition	CPC	CPL	CPU	CSC
Design	3	-11	-12	-13	Design	4	-6	-10	-30
Ballast	-17	-11	-2	-23	Ballast	-14	-20	-14	-18
Average Pitch Angle (deg)					Average Pitch Angle (deg)				
Condition	CPC	CPL	CPU	CSC	Condition	CPC	CPL	CPU	CSC
Both	-7	-11	-7	-18	Both	-5	-11	-12	-24
Optimal Flap Angle (deg)					Optimal Flap Angle (deg)				
Condition	FPC	FPL	FPU	FSC	Condition	FPC	FPL	FPU	FSC
Design	7	-5	7	-9	Design	2	-8	0	0
Ballast	-13	0	2	1	Ballast	-8	-10	-8	0

Table 8 Model Test and CFD Optimized Angle Results

The finally obtained pitch angles and flap angles in the tank tests are summarized in Table 8. In spite of some fluctuations during the tests, the agreement between CFD and model tests are considered satisfactory. Generally, most of the CFD determined optimum fin pitch angles were well validated by the tank tests, while the optimum flap angles were in less agreement.

According to the model tests results, the full scale's performance was predicted using FORCE Technology's extrapolation method. Figure 4 shows the RPM values comparison at different ship speeds. It can be seen that the RPM decreases about 3% for all the cases with CPSF. This is in line with the previous CFD calculations.

As shown in Figure 5, the CPSF device reduces the shaft power by 2.8 to 3.5% at design draft and 2.6 to 4% at ballast draft.

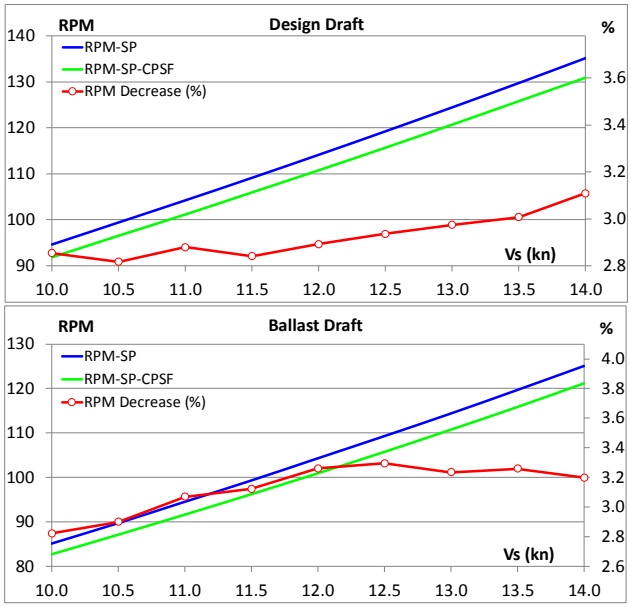

Figure 4 RPM at Different Ship Speeds

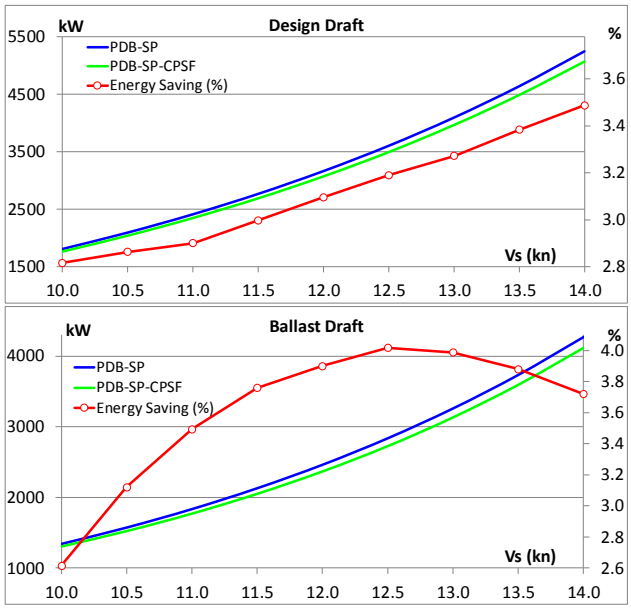

Figure 5 P_{DB} at Different Ship Speeds

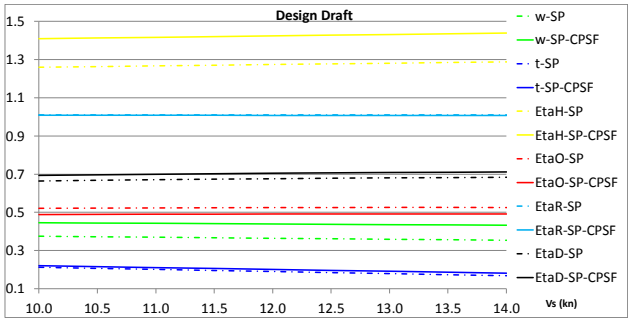

Figure 6 Propulsion Factors at Design Draft

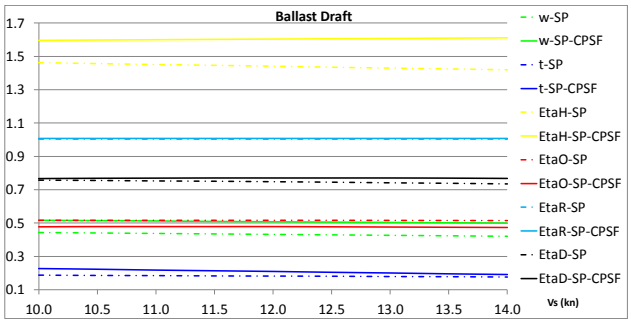

Figure 7 Propulsion Factors at Ballast Draft

Figure 6 and Figure 7 depict the propulsion factors at different ship speeds at design and ballast draft, respectively. For the CPSF the propeller has in all cases a slightly lower open water efficiency (η_o) due to an increased effective wake and hence higher propeller loading. The relative rotational efficiency η_R in the CPSF case is roughly identical in both design and ballast drafts. The thrust deduction with CPSF is clearly increased. Despite the slightly higher trust deduction, the higher effective wake for the CPSF case leads to better hull efficiency and thus a better total efficiency in the speed range tested.

In order to make the parallel comparisons, the obtained optimal CPSF configurations from tank tests were applied directly to the CFD solver, both in model and full scale at these two conditions, to get the corresponding CFD results. By doing so, the CFD solver itself could be validated. More importantly, the flow details, which cannot be measured by the tank tests, could be investigated to find the working principle of CPSF.

It is well known that in the self-propulsion CFD calculation using Rigid Body Motion (RBM) method, the result will be somewhat dependent on the selected time step. During the entire CFD optimization, it was set to 6 degrees per time step to save on computation time. After completion of the model tests it was decided to include a time step analysis for verifying its influence on the accuracy of the CFD results. In addition to the 6 degree time step, two other time steps, 3 degree and 1 degree were used to investigate its influence. If the total propulsion efficiency and shaft power used as comparison, it can be found that the smaller the time step is, the smaller the deviations are. Time step's influence on the energy saving are listed in Table 9. It can be seen when compared with the tank test's energy saving percentages, the previously adopted 6 degrees per time step will underestimate these values by about 2%. For the reason that 1 degree per time step would make the calculation time very long, 3 degrees time step size was adopted in the following full scale's validation and comparison.

Condition	P_{DB} (W)	6Deg	3Deg	1Deg	FORCE-2018
Design	SP	2868620	2828586	2815183	2769000
	SP-CPSF	2843385	2767096	2744108	2686000
	Saving (%)	-0.88	-2.17	-2.52	-3.00
Ballast	SP	2633516	2630480	2625146	2461000
	SP-CPSF	2578351	2531239	2526906	2365000
	Saving (%)	-2.09	-3.77	-3.74	-3.90

Table 9 Time Step Size's Influence on Energy Saving

	CFD	J	η_O	η_R	η_H	η_D	P_{DB} (W)
Design Condition	SP	0.4272	0.5459	1.0279	1.1734	0.6584	2828586
	SP-CPSF	0.3805	0.5066	1.0188	1.3233	0.6830	2767096
	Dev (%)	-10.93	-7.20	-0.89	12.77	3.74	-2.17
	FORCE-2018	J	η_O	η_R	η_H	η_D	P_{DB} (W)
	SP	0.3960	0.5240	1.0110	1.2710	0.6740	2769000
	SP-CPSF	0.3602	0.4900	1.0090	1.4200	0.7020	2686000
	Dev (%)	-9.04	-6.49	-0.20	11.72	4.15	-3.00
	Diff of Dev%	1.89	0.71	0.69	-1.05	0.42	-0.82
Ballast Condition	CFD	J	η_O	η_R	η_H	η_D	P_{DB} (W)
	SP	0.4335	0.5506	1.0278	1.2287	0.6953	2630480
	SP-CPSF	0.3921	0.5171	1.0221	1.3730	0.7257	2531239
	Dev (%)	-9.55	-6.08	-0.55	11.74	4.37	-3.77
	FORCE-2018	J	η_O	η_R	η_H	η_D	P_{DB} (W)
	SP	0.3880	0.5170	1.0040	1.4410	0.7480	2461000
	SP-CPSF	0.3478	0.4780	1.0070	1.6040	0.7710	2365000
	Dev (%)	-10.36	-7.54	0.30	11.31	3.07	-3.90
	Diff of Dev%	-0.81	-1.46	0.85	-0.43	-1.30	-0.13

Table 10 Relative Comparison with Tank Test Data

Table 10 lists the relative values comparison with the tank test data when using a 3-degree time step. Even though the absolute values of η_O and η_H obviously deviate, the relative deviations between without and with CPSF are very close. Most of them are around 1%. This means, that even though the absolute deviations are obvious for some parameters, the influence of CPSF to the system's hydrodynamic parameters are captured accurately.

Model Scale	P_{DB} at Design Draft			P_{DB} at Ballast Draft		
Speed (kn)	SP (W)	SP-CPSF (W)	Saving (%)	SP (W)	SP-CPSF (W)	Saving (%)
10.0	31.804	30.856	-3.0	23.149	22.742	-1.8
11.0	42.964	41.665	-3.0	32.538	31.435	-3.4
11.5	48.955	47.737	-2.5	38.081	36.357	-4.5
12.0	55.997	54.343	-3.0	43.802	41.672	-4.9
13.0	72.162	70.272	-2.6	56.574	55.100	-2.6
14.0	91.199	88.194	-3.3	74.612	72.216	-3.2

Table 11 Energy Savings at Different Ship Speeds

Table 11 shows the energy savings at different ship speeds as obtained from the model tests with the final fin configuration. Again, it can be noticed that at the design condition (Vs = 11.5 kn), the energy saving is only 2.5%, which is lower than the value obtained during the optimization stage. This somehow underlines the initial expectation that the model tests optimization could be difficult to perform with sufficient accuracy, even though FORCE Technology did their best to eliminate all uncertainties.

The fins were then removed one by one to see their contributions to the energy saving. When tested with fins removed one by one after optimization tests, both ballast and design results suggest that the main contribution to the power gains comes from SC fin, as shown in Table 12. The ranking of each fin's contribution to the total energy saving is SC > PL > PC > PU.

	Design Condition			Ballast Condition		
	Saving (%)	Loss (%)	Rank	Saving (%)	Loss (%)	Rank
SP-CPSF	-4.3			-5.5		
No-PC	-3.4	-20.9	3	-4.7	-14.5	3
No-PL	-2.9	-32.6	2	-4.6	-16.4	2
No-PU	-4.2	-2.3	4	-4.9	-10.9	4
No-SC	-2.1	-51.2	1	-1.5	-72.7	1

Table 12 Energy Savings with One Fin Removed

Then the obtained optimal CPSF configurations from tank tests at these two conditions were applied directly to CFD solver in model scale to make the parallel comparisons. First of all, the nominal wake field was validated using different turbulence models including SST k-w, k-e V2F and Reynolds Stress Model with Quadratic Pressure Strain (RSM-QPS). It's found that the RSM-QPS has the best prediction ability. SST k-w and k-e V2F models have the same level performance. For the computation cost, the more turbulence equations that are included, the longer the computation time is. Thus, RSM-QPS (6-equation model) is the most time consuming model, and SST k-w (2-equation model) uses the least time, k-e V2F (4-equation model) lies somewhere between them. However, RSM-QPS cannot predict very well hull resistance result. What's more, this model's convergence process is not stable. Thus, SST k-w and k-e V2F turbulence were used for the following validation. After several rounds of tuning with also the wall Y+ value being considered, the best agreement with the measured data can be obtained, as listed in Table 13. Even though some of the parameters still have the deviations above 5%, most of them are already in the acceptable level, especially if judging from the total propulsion efficiency η_D and the shaft power P_{DB}.

Design Condition	RPS	1-t	1-w	J	η_O	η_R	η_H	η_D	P_{DB} (W)
SP-CFD	8.3888	0.8870	0.6199	0.3972	0.5216	0.9942	1.4308	0.7420	49.3797
SP-FORCE-2018	8.3280	0.8527	0.5848	0.3774	0.5037	1.0144	1.4581	0.7451	48.8203
Dev (%)	0.73	4.02	6.01	5.24	3.54	-1.99	-1.87	-0.42	1.15
Design Condition	RPS	1-t	1-w	J	η_O	η_R	η_H	η_D	P_{DB} (W)
SP-CPSF-CFD	8.1807	0.8638	0.5525	0.3630	0.4899	0.9912	1.5634	0.7592	48.3863
SP-CPSF-FORCE-2018	8.1044	0.8357	0.5122	0.3397	0.4666	1.0130	1.6315	0.7711	47.6117
Dev (%)	0.94	3.36	7.86	6.86	5.00	-2.16	-4.18	-1.55	1.63
Ballast Condition	RPS	1-t	1-w	J	η_O	η_R	η_H	η_D	P_{DB} (W)
SP-CFD	7.9160	0.8446	0.5175	0.3667	0.4935	0.9714	1.6321	0.7824	44.4921
SP-FORCE-2018	7.9945	0.8386	0.5308	0.3724	0.4990	1.0101	1.5798	0.7963	43.7007
Dev (%)	-0.98	0.72	-2.50	-1.54	-1.10	-3.83	3.31	-1.74	1.81
Ballast Condition	RPS	1-t	1-w	J	η_O	η_R	η_H	η_D	P_{DB} (W)
SP-CPSF-CFD	7.6943	0.8527	0.4743	0.3457	0.4727	0.9799	1.7977	0.8328	41.7514
SP-CPSF-FORCE-2018	7.6854	0.8155	0.4451	0.3248	0.4511	1.0104	1.8321	0.8350	41.5767
Dev (%)	0.12	4.56	6.56	6.44	4.80	-3.01	-1.88	-0.27	0.42

Table 13 Model Scale's Validations

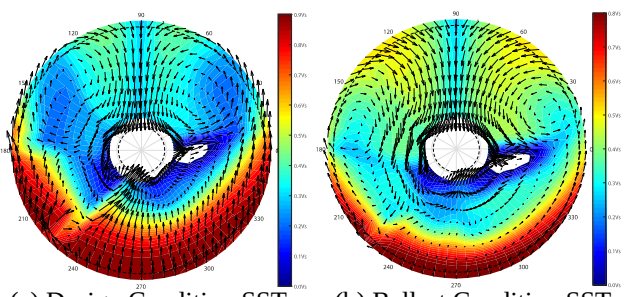

(a) Design Condition SST (b) Ballast Condition SST

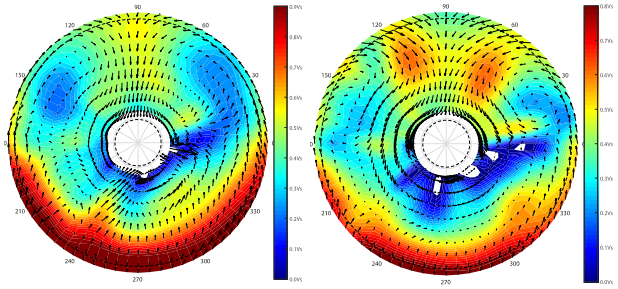

(c) Design Condition Test (d) Ballast Condition Test

Figure 8 Nominal Wake Comparison of CFD and Test

Figure 8 is the nominal wake comparison using CFD with SST k-w and test at design and ballast condition with CPSF. Generally, the CFD predictions can capture the main characteristics of the wake fields. However, some difference can still be noticed if the upper area is considered. The influence of CPSF to the wake field can be seen very clearly, except the port side upper fin. After further investigations of the flow field near all the fins, it can be found that PU fin has the lowest influence to the wake. As listed in Table 12, PU fin makes also the lowest contribution to the total energy savings.

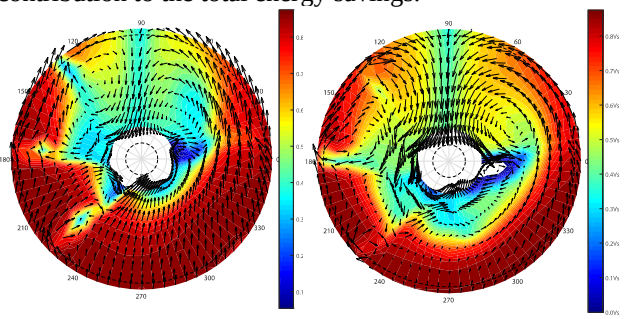

(a) Design Condition SST (b) Ballast Condition SST

Figure 9 Nominal Wake with CPSF in Full Scale

Figure 9 is the nominal wake with CPSF in full scale. The low speed area in the wake field at model scale (Figure 8 (a) and (b)) is larger than that of full scale. However, PU fin seems to have a more pronounced influence on the wake field in full scale than that in model scale. This indicates that the scale effect cannot be neglected. It is recommended from this study to make the CFD optimization of CPSF in full scale, considering the final application.

8 WAKE KINETIC ENERGY ANALYSIS

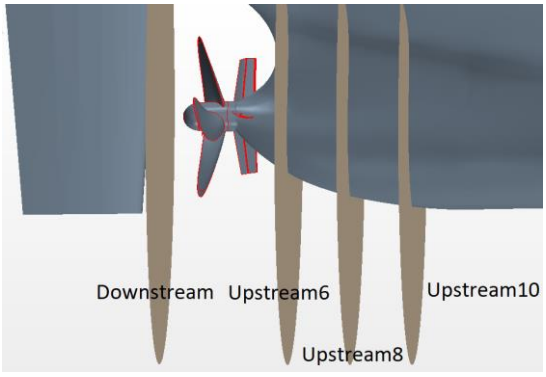

Figure 10 Sections for Kinetic Energy Analysis

In order to analyze the kinetic energy in the hull wake, four sections across the hull are selected as shown in Figure 10. Their locations are at 10 m, 8 m, 6 m and 1.85 m upstream of aft perpendicular i.e. three sections in front of the propeller and one aft. Then the kinetic energy in axial and transverse directions through any of the section per second can be calculated using the following formulas:

$$E_{ax} = 0.5\rho\int V_a \left(V_S - V_a\right)^2 \mathrm{d}S \quad (1)$$

$$E_{tr} = 0.5\rho\int V_a \left(V_r^2 + V_t^2\right) \mathrm{d}S \quad (2)$$

$$E_{total} = E_{ax} + E_{tr} \quad (3)$$

Here, V_a, V_r and V_t are the axial, radial and tangential velocities.

Figure 11 and Figure 12 plot the development of time-averaged kinetic energy in axial and transverse direction through these four sections at design and ballast conditions. It can be noticed that from section upstream10 to upstream6, the kinetic energy is not constant. At design condition without and with CPSF, the total kinetic energy increases as the flow approaching the propeller. However, this tendency is different for the ballast condition without and with CPSF. For all cases, the axial kinetic energy increases and the transverse kinetic energy decreases as the flow approaching the propeller plane. The CPSF's influence is very limited at the selected upstream sections. At the downstream section, the values of kinetic energy in axial and transverse directions are very close for the cases without CPSF. With CPSF, the axial kinetic energy decreases a little but the transverse kinetic energy decreases significantly. Thus, the total kinetic energy with CPSF is remarkably reduced compared with the cases without CPSF at this downstream location. Table 14 lists the kinetic energy changes from upstream to downstream. As shown in Table 14, CPSF has lowered the total kinetic energy in the wake field by 113318 J per second at design condition and 119053 J per second at ballast condition, among which, less than 10% coming from the axial direction. The saved shaft powers are 54.3% and 83.4% of the recovered kinetic energy at design and ballast condition respectively.

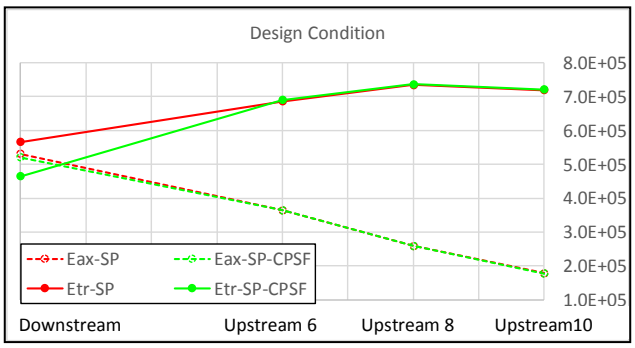

Figure 11 Development of Kinetic Energy in Axial and Transverse Direction at Design Condition

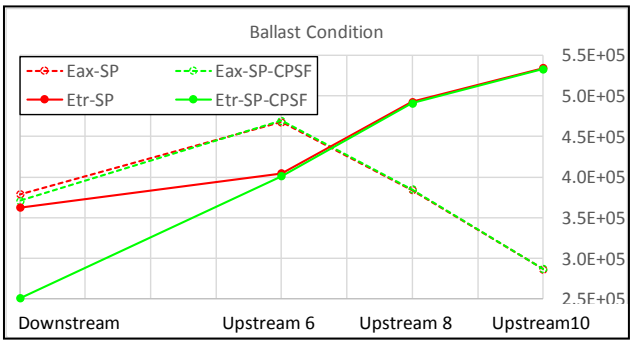

Figure 12 Development of Kinetic Energy in Axial and Transverse Direction at Ballast Condition

Full Scale-CFD	Design Condition (W)			Ballast Condition (W)		
Δ	SP	SP-CPSF	Diff	SP	SP-CPSF	Diff
ΔEax	352934	342575	-10360	92234	83571	-8664
ΔEtr	-152865	-255823	-102958	-171888	-282277	-110389
ΔEtotal	200069	86752	-113318	-79653	-198706	-119053
P_{DB}	2828586	2767096	-61490	2630480	2531239	-99241
P_{DB}/ΔEtotal (%)			54.3			83.4

Table 14 Kinetic Energy Results through Sections

9 CONCLUSIONS

In this paper, the whole process of the CPSF's CFD validation, optimization and tank test validation both in model and full scale is presented. More detailed results and analysis can be found in Jin et al (2019). By analyzing the corresponding results, the following conclusions can be obtained:

1) The CFD solvers in model and full scale were validated against the tank test data. Even though the absolute deviations are present, differences of the relative deviations without and with CPSF are mostly within 1%. This proves that CFD and the selected solvers are good enough to capture the fins' influence to the propulsion performance.

2) The optimum fin configurations at full scale and model scale were different. The optimal angles at model scale are obviously larger than those at full scale, because of the different in the boundary layers at model and full scale.

3) The CFD determined optimum fin pitch angles were well validated by the tank tests, while the optimum flap angles were in less agreement.

4) The individual fins contributed unevenly to the total savings. The starboard center fin proved to be the most effective one, no matter whether determined by CFD calculation or tank tests.

5) The fins' net energy savings mainly originated from an increased hull efficiency, even though the propeller efficiency turned out to be slightly lower.

6) The energy gain comes mainly from the recovery of the rotational loss in the wake field.

7) CPSF can lead to savings of the delivered shaft power by about 3-4% in case of the selected bulk carrier at both conditions.

8) Considering the obvious difference of the model and full scale wake fields, it is recommended to optimize CPSF in full scale.

10 ACKNOWLEDGEMENT

This project is financially supported by the Danish government Blue INNOship initiative (http://www.blaainno.dk).

The project consortium consists of the partners

- Maersk Line
- Technical University of Denmark, DTU-MEK
- OSK-ShipTech
- MAN Energy Solutions

The project will be finalized in April 2019 after concluding a design of a CPSF wake adapted propeller and model testing of this configuration.

REFERENCES

Kim, M. C., Chun, H. H. & Kang Y.D. (2004). 'Design and Experimental Study on a New Con-cept of Preswirl Stator as an Efficient Energy-Saving Device for Slow Speed Full Body Ship', SNAME Annual Meeting

Nielsen, J.R., Sørensen, K.B. & Nørgaard, H.H. (2013). 'Design and optimisation of fuel-efficient propulsion systems', Motorship Conference

Kim, K., Leer-Andersen, M., Werner, S., Orych, M. & Choi, Y. (2013). 'Hydrodynamic optimization of pre-swirl stator by CFD and model testing', International Shipbuilding Progress 60:233–276

Jin, W. & Nielsen, J.R. (2019), 'Development of Controllable Pre-Swirl Fins Adapted to Different Operation Conditions', MAN Internal Report